

What Is the Origin of the Contrathermodynamic Behavior in Methyl Radical Addition to Alkynes versus Alkenes?

Rodolfo Gómez-Balderas,^{†,‡,§} Michelle L. Coote,^{*,†} David J. Henry,[†] Hanns Fischer,^{||} and Leo Radom^{*,†,§}

Research School of Chemistry, Australian National University, Canberra, ACT 0200, Australia, School of Chemistry, University of Sydney, Sydney, NSW 2006, Australia, and Physikalisch-Chemisches Institut der Universität Zürich, Winterthurerstrasse 190, 8057 Zürich, Switzerland

Received: April 17, 2003; In Final Form: June 4, 2003

High-level *ab initio* calculations of the barriers, enthalpies, and rate constants have been performed for methyl radical addition to ethyne, propyne, ethene, and propene. We find that addition to alkenes is kinetically favored over addition to alkynes, despite the larger exothermicity of the alkyne addition reactions. The results have been rationalized using the curve-crossing model. To this end, the singlet–triplet gaps and charge-transfer energies in the reactants, and the extent of charge separation in the transition structures, have been calculated. It is concluded that the greater barrier for addition to alkynes is primarily the result of the larger singlet–triplet gap in the substrate. This barrier-raising effect dominates the barrier-lowering effect of the reaction exothermicity.

1. Introduction

The addition of alkyl radicals to multiple bonds is of fundamental importance as a carbon–carbon bond-forming reaction. Addition to C=C bonds has received widespread attention, but there have been relatively few studies of addition to C≡C bonds.^{1,2}

An intriguing observation has been that the barrier for addition to alkynes is slightly greater than that for addition to alkenes, despite the greater exothermicity in the former case.¹ For the prototypical systems, methyl addition to ethene and ethyne, this is found in both solution-phase³ and gas-phase⁴ experiments, with the difference in the barriers being approximately 2–3 kJ/mol. This difference in barriers is increased to ~5 kJ/mol if a more-recent estimate for the barrier for addition to ethene is used in the comparison.¹ In contrast, the estimated frequency factors favor addition to ethyne over addition to ethene. These competing enthalpic and entropic effects have led to the prediction that the relative reaction rates might be temperature sensitive, with the solution-phase study³ (performed over the range of 328–358 K) predicting that addition to ethene is faster and the gas-phase study⁴ (at 379–487 K) finding the reverse. However, when the solution- and gas-phase Arrhenius parameters are used to predict the rate constants for methyl radical addition to ethene and ethyne at the same temperature (298 K), contradictory results are obtained, with the solution-phase results predicting that addition to ethene is faster by a factor of 1.5 and the gas-phase data predicting that addition to ethyne is favored by a similar amount.¹

The observation that the barrier for radical addition to ethyne is greater than that to ethene, despite the greater exothermicity in the former case, has been supported by density functional

theory calculations by Barone and Orlandini.⁵ Building on an earlier study,⁶ they also predicted that the opposing enthalpic and entropic effects should lead to a crossing in the rate constants at ~400 K. In addition, the gas-phase kinetics for addition to ethyne have been reproduced reasonably accurately with the higher-level BAC-MP4 calculations⁷ of Diau et al.⁸

The contrathermodynamic preference for radical addition to alkenes over alkynes has also been observed for the addition reactions involving substituted carbon-centered radicals and/or substituted substrates. For example, in a recent review of radical addition reactions,¹ solution-phase rate constants at 298 K for the addition of methyl radical, *tert*-butyl radical, and *tert*-butoxycarbonyl methyl radical to correspondingly substituted alkenes and alkynes were compared, for a range of substituents, including methyl, phenyl, SiMe₃, CO₂Me, and CO₂Et. In all cases, the rate constant for addition to the alkene is greater than that for the corresponding alkyne, by factors of up to 1 order of magnitude (though generally differences of a factor of 2–6 are observed). Where Arrhenius parameters were reported, the preference for addition to the alkenes was again a result of a lower reaction barrier (with the frequency factors either being similar or favoring addition to the alkynes). Interestingly, in contrast to the prototypical systems, the kinetic preference for methyl radical addition to alkenes over alkynes for the methyl-substituted substrates (i.e., propene and propyne) is found both in the gas phase and in solution.

Various alternative qualitative rationalizations for this contrathermodynamic preference for methyl radical addition to alkenes over alkynes (at least at lower temperatures) have been proposed. In early work, Gazith and Szwarc⁹ suggested that the increased activation energy in the addition to alkynes was due to the stronger interaction of the π -electrons in the shorter C≡C bond compared with the C=C bond. More recently, Nicolaides and Borden¹⁰ calculated the relative bond strengths of the π -bonds in acetylene and ethylene, and confirmed that the former bond was indeed stronger. In contrast to the arguments based on bond strength, Barone et al.^{5,6} used a Morokuma-type

* To whom correspondence should be addressed. E-mail: mcoote@rsc.anu.edu.au and radom@chem.usyd.edu.au.

[†] Australian National University.

[‡] On postdoctoral leave from FESC-UNAM (México).

[§] University of Sydney.

^{||} Physikalisch-Chemisches Institut der Universität Zürich.

analysis^{11,12} to compare the barriers for addition to ethene and ethyne, and concluded that the increased barrier for addition to the alkyne arose because of the greater geometrical deformation of the transition structure for this reaction. An alternative rationalization, using the curve-crossing model,^{13,14} has been presented by Fischer and Radom,¹ who attributed the lower reactivity of the alkyne partly to its larger singlet–triplet gap, and partly to a higher ionization energy and lower electron affinity.

In the study presented here, we aim to enhance our understanding of these fundamental reactions in several ways. First, we use state-of-the-art calculations that have been found to be appropriate for the theoretically difficult radical addition reactions¹⁵ to compare methyl radical addition to alkenes and alkynes. Second, we include calculations on both the unsubstituted and methyl-substituted systems. Finally, we calculate the quantities such as ionization energies, electron affinities, and triplet excitation energies that are required for an analysis using the curve-crossing model. In this way, we hope to establish definitively whether radical addition to alkenes is kinetically favored over addition to alkynes at normal temperatures, and to determine why the barrier for radical addition to alkynes is higher than that for addition to alkenes, despite the greater exothermicity in the former case.

2. Theoretical Procedures

Standard *ab initio* molecular orbital theory¹⁶ and density functional theory¹⁷ calculations were carried out using the GAUSSIAN 98¹⁸ and MOLPRO 2000.6¹⁹ programs. Barriers and enthalpies were calculated for methyl radical addition to ethene, propene, ethyne, and propyne. Geometries of reactants, products, and transition structures were optimized at the UQCISD/6-31G(d) level of theory, and zero-point energies were calculated using frequencies obtained at the same level, scaled by a factor of 0.9776.²⁰ Improved energies were calculated using the W1h variant²¹ of the W1 theory of Martin et al.^{22,23} This is a high level of theory that aims to approximate coupled cluster [URCCSD(T)] results with an infinite basis set using extrapolation procedures. Corrections are also included for scalar relativistic effects and core correlation, and for spin–orbit coupling in atoms. In the W1h variant of W1 theory, nonaugmented basis sets are used for both carbon and hydrogen. It should be noted that the method used in this work is effectively a modification of standard W1h theory, in that the lower-level UB3-LYP/cc-pVTZ geometries and zero-point vibrational energies are replaced by more accurate¹⁵ UQCISD/6-31G(d) calculations. We refer to this as W1h//QCISD/6-31G(d). An assessment of the performance of this and other levels of theory for the study of methyl radical addition to alkenes and alkynes will be published separately.¹⁵ However, it may be noted that the estimated uncertainty in W1 theory (based on comparison with a test set of experimental heats of formation for 55 stable molecules²¹) is 2.5 kJ/mol.

Frequency factors and rate constants for the various addition reactions were calculated via simple transition state theory using scaled (by 1.0187²⁰) UQCISD/6-31G(d) frequencies. In calculation of the entropy of activation, the low-frequency torsional modes were treated as hindered rotors. The rotational potentials associated with these modes were obtained at the UQCISD/6-31G(d) level of theory, and the corresponding partition functions and associated thermodynamic properties were then determined via standard methods as follows. For those modes having rotational potentials that could be described by a simple cosine function, the tables of Pitzer and co-workers^{24,25} were

used. For the more complex modes, the rotational potentials were fitted with a Fourier series of up to 18 terms, and the corresponding energy levels were then found by numerically solving the one-dimensional Schrödinger equation for a rigid rotor using a Fortran program described previously.^{26,27} The hindered rotor model, in conjunction with scaled (by 1.0080²⁰) UQCISD/6-31G(d) frequencies, was also employed in the calculation of temperature corrections to the barriers and reaction enthalpies.

The curve-crossing model^{13,14} was used to provide a qualitative rationalization of the contrasting behavior of methyl radical addition to alkenes and alkynes, and this required various additional quantities to be calculated. These include vertical ionization energies (IEs) and electron affinities (EAs) for the reactants, and the vertical singlet–triplet excitation gaps for the alkene and alkyne substrates. These quantities were calculated at the G3X(MP2)-RAD level of theory.^{28,29} The extent of charge transfer in the transition structures was established by calculating Bader charges via atoms-in-molecules (AIM) calculations.³⁰ These were performed in GAUSSIAN at the UQCISD/6-31G(d) level of theory using the correlated (rather than SCF) wave function to calculate the electron density.

3. Results and Discussion

Calculated barriers (ΔH^\ddagger_0) and enthalpies (ΔH_0) for methyl radical addition to alkynes ($\text{CH}\equiv\text{CX}$, where X is H or CH_3) and alkenes ($\text{CH}_2=\text{CHX}$, where X is H or CH_3) at 0 K are shown in Table 1. Also included in Table 1 are the calculated reaction enthalpies (ΔH_{298}) and rate constants (k_{298}) at 298 K, along with the corresponding Arrhenius parameters, E_{a298} and $\log(A_{298})$.³¹ Selected experimental data^{1,32,33} are included in Table 1 for purposes of comparison.

Our results confirm the earlier observations^{1,5,6} that methyl radical addition to alkynes has a considerably higher reaction barrier, despite being more exothermic. In the work presented here, we find that the exothermicities favor addition to the triple-bonded substrates by 6.9 kJ/mol for the unsubstituted system and 7.3 kJ/mol for the methyl-substituted system (at 298 K). In contrast, the corresponding Arrhenius activation energies at 298 K favor addition to the alkenes by 8.4 and 8.3 kJ/mol for the unsubstituted and methyl-substituted systems, respectively. Although the frequency factors (at 298 K) favor addition to the alkynes, methyl radical addition to alkenes is nonetheless kinetically favored (by factors of 8 and 15, respectively) because of the considerably smaller reaction barriers. This contrathermodynamic preference for addition to alkenes over alkynes is in accordance with the available solution-phase experimental data^{1,3} for both the methyl-substituted and unsubstituted systems, and the gas-phase data^{1,4} for the methyl-substituted systems, but not the gas-phase data^{1,4} for the unsubstituted systems.

It can also be seen from Table 1 that the effects of methyl substitution on the barriers and enthalpies of the two pairs of addition reactions are relatively small. However, the effect of methyl substitution on the frequency factors (and therefore the rate constants) is larger, with factors of approximately 0.3 and 0.2 being calculated for the alkenes and alkynes, respectively. These effects are mainly due to differences in the reaction path degeneracy, though in the case of the alkynes, a more direct methyl substituent effect does serve to decrease the frequency factor by an additional factor of approximately 2. Nonetheless, the effect of methyl substitution on the comparative behavior of the alkenes and alkynes is relatively minor, and hence, for the remainder of this work, we focus mainly on methyl radical addition to the parent systems, ethene and ethyne.

TABLE 1: Calculated Kinetic and Thermodynamic Parameters for Methyl Radical Addition to $\text{CH}\equiv\text{CX}$ and $\text{CH}_2=\text{CHX}$ (where X is H or CH_3) at 0 and 298 K^a

reaction	ΔH^\ddagger_0	ΔH_0	ΔH_{298}	E_{a298}	$\log(A_{298})$	$\log(k_{298})$
$\bullet\text{CH}_3 + \text{CH}\equiv\text{CH}$	47.1	-95.5	-103.5	45.8	9.2	1.2
gas-phase experiment ^b	—	—	-106.9 ± 7 ^c	32.2/36.2	8.8	3.1 ± 0.5
solution-phase experiment ^b	—	—	—	34.3/33.2	9.7	3.7
$\bullet\text{CH}_3 + \text{CH}\equiv\text{CCH}_3$	45.9	-97.0	-103.7	45.1	8.5	0.6
gas-phase experiment ^b	—	—	—	36.8/39.6	8.7	2.3
solution-phase experiment ^b	—	—	—	31.1/33.4	8.8	3.3
$\bullet\text{CH}_3 + \text{CH}_2=\text{CH}_2$	37.9	-90.5	-96.6	37.4	8.7	2.1
gas-phase experiment ^b	—	—	-98.8 ± 3 ^c	30.8/33.5	8.3	2.9 ± 0.3
solution-phase experiment ^b	—	—	—	31.4/28.2	9.3	3.8
$\bullet\text{CH}_3 + \text{CH}_2=\text{CHCH}_3$	36.4	-91.0	-96.4	36.8	8.2	1.7
gas-phase experiment ^b	—	—	-98.7 ± 3 ^c	29.7/33.1	7.9	2.7
solution-phase experiment ^b	—	—	—	32.3/27.7	9.3	3.6

^a Energies in kilojoules per mole and A and k in liters per mole per second. Calculated at the W1h//QCISD/6-31G(d) level of theory (see the text). ^b All experimental numbers taken from ref 1 (and references therein) unless noted otherwise. As in ref 1, two experimental estimates are provided for each Arrhenius activation energy. The first entry refers to the reported value from the original work and the second to a reanalysis of the rate data assuming $\log(A) = 8.5$ per $\text{CH}_2=$ group for addition to the alkenes and $\log(A) = 9.2$ per $\text{CH}\equiv$ group for addition to alkynes. ^c Calculated using experimental heats of formation taken from ref 32 for the radicals (CH_3^\bullet , $\text{CH}_3\text{CH}_2\text{CH}_2^\bullet$, and $\text{CH}_3\text{CH}=\text{CH}^\bullet$) and from ref 33 for all other species.

Comparison of the experimental and theoretical data in Table 1 shows that there is excellent correspondence between theory and experiment for the reaction enthalpies. Furthermore, the *trends* in the experimental rate constants (with respect to both the alkene vs alkyne difference and the methyl substituent effect) are generally in accord with our calculations. However, anomalies are observed in the case of the gas-phase experimental data for addition to the alkynes.^{1,4} For these systems, the experimental results were obtained prior to the development of techniques that are capable of measuring the rates of radical addition reactions directly, and a reinvestigation using contemporary procedures would therefore be desirable.

In the case of addition to the alkenes, the gas-phase experimental rate constants differ from the calculated values by just less than 1 order of magnitude, and this is probably a reasonable estimate of the combined uncertainties in both. However, there are somewhat larger differences between the calculated rate constants and the solution-phase^{1,3} values. These discrepancies reflect more fundamental issues that are relevant to comparisons of the calculated rate constants (which correspond to those of an ideal gas at its high-pressure limit) with the solution-phase experimental data. These will be discussed in more detail in a forthcoming assessment of theoretical procedures for these systems.¹⁵ For the present, it may be noted that *experimental* solution-phase and gas-phase rate constants for radical addition reactions generally differ by 1 order of magnitude,¹ and this may obscure some of the quantitative comparisons between the calculated results and the experimental solution-phase data.

The results presented here confirm that methyl radical addition to alkenes and alkynes is contrathermodynamic. To illustrate this further, rate constants for methyl addition to ethene and ethyne are plotted as a function of temperature in Figure 1, where it can be seen that addition to ethene is favored over a wide temperature range. In a previous theoretical study of these systems, Barone and Orlandini⁵ predicted that, while addition to ethene should be favored at low temperatures, the rate constants should cross at ~ 400 K because of the competing enthalpic and entropic effects. In the present work, we do not observe this crossing because the differences in the reaction barriers are calculated to be larger and the differences in frequency factors are calculated to be smaller at the current high level of theory. This moves the *expected* "crossing point" to significantly higher temperatures. This can be seen in Figure 2,

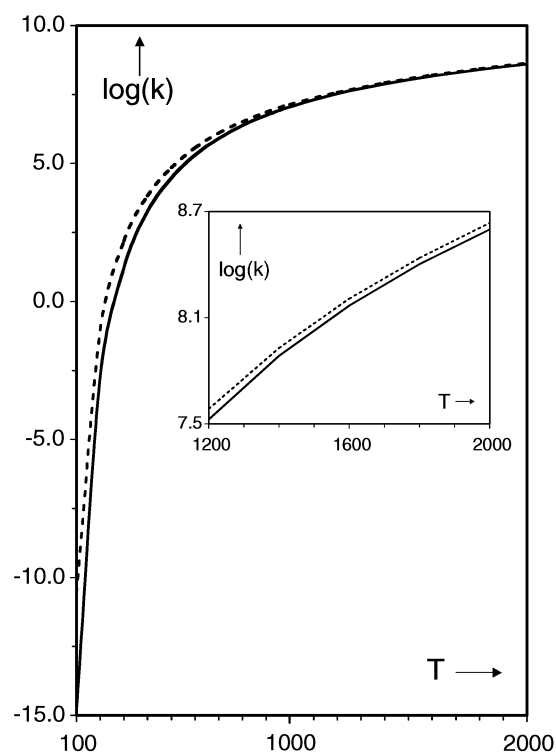


Figure 1. Calculated rate constants (k , in liters per mole per second) for methyl radical addition to $\text{CH}\equiv\text{CH}$ (—) and $\text{CH}_2=\text{CH}_2$ (- - -) as a function of temperature (T , in kelvin) using W1h energies in conjunction with geometries and frequencies obtained at the UQCISD/6-31G(d) level.

where the enthalpies (ΔH^\ddagger), entropies (plotted as $-T\Delta S^\ddagger$), and Gibbs free energies (ΔG^\ddagger) of activation for methyl radical addition to ethene and ethyne are plotted as a function of temperature. From these results, it is seen that the difference in ΔG^\ddagger for addition to ethene and ethyne is dominated by the difference in ΔH^\ddagger up to quite high temperatures.

Interestingly, however, even at high temperatures, the crossing in the rate constants does not occur because at high temperatures the entropies themselves cross, with addition to ethene becoming the entropically favored reaction. The crossing in the entropies of activation is the result of competing effects. The rotational contribution to the entropy of activation favors addition to the (linear) ethyne, as it has one less rotational degree of freedom to lose upon reaction. In contrast, the vibrational contribution

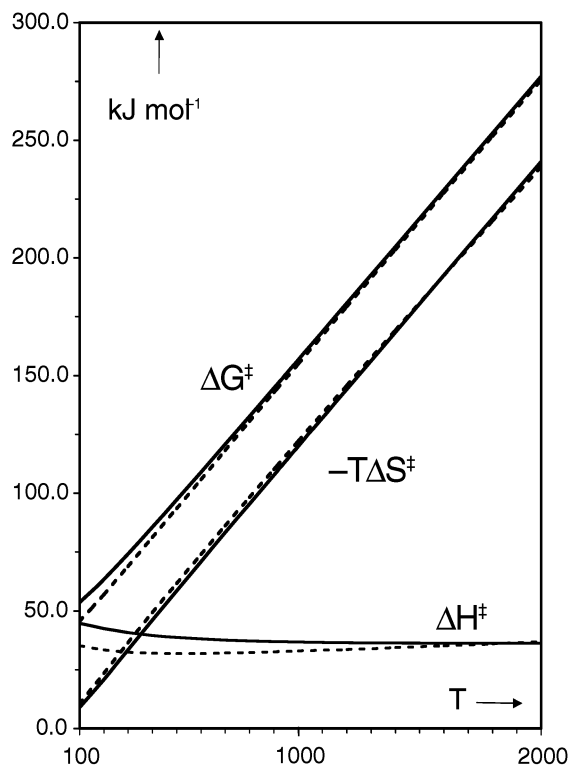


Figure 2. Free energies of activation (ΔG^\ddagger , in kilojoules per mole) and their enthalpic (ΔH^\ddagger , in kilojoules per mole) and entropic ($-T\Delta S^\ddagger$, in kilojoules per mole) contributions, calculated as a function of temperature (T , in kelvin) for methyl radical addition to $\text{CH}\equiv\text{CH}$ (—) and $\text{CH}_2=\text{CH}_2$ (---). Values derived from W1h energies in conjunction with geometries and frequencies obtained at the UQCISD/6-31G(d) level.

favors addition to the (more “floppy”) ethene. At low temperatures, the difference in ΔS^\ddagger is dominated by the rotational contribution, but as the temperature increases, the difference in the vibrational contribution to ΔS^\ddagger increases at a faster rate, and eventually dominates the difference in ΔS^\ddagger for the two reactions. Thus, at low temperatures, the (rotationally favored) addition to ethyne is the entropically favored reaction, while at high temperatures, the (vibrationally favored) ethene addition is favored (see Figure 3).

Methyl radical thus adds to triple bonds with a higher reaction barrier and a slower rate constant compared with addition to double bonds, despite the former being a more exothermic process. In what follows, we attempt to explain this observation by means of an analysis using the curve-crossing model. Before proceeding to this discussion, however, we compare briefly the transition structure geometries for the various addition reactions.

Geometries. Transition structure geometries (**1b–4b**) for methyl radical addition to alkynes ($\text{CH}\equiv\text{CX}$, where X is H or CH_3) and alkenes ($\text{CH}_2=\text{CHX}$, where X is H or CH_3) are shown in Figure 4. The geometries of the corresponding alkenyl and alkyl product radicals are included for purposes of comparison. The key geometrical parameters for all of these species, obtained at the UQCISD/6-31G(d) level of theory, are listed in Table 2, while complete geometries in the form of GAUSSIAN archive entries are provided in Table S1 of the Supporting Information. Results for both cis and trans conformations of the alkenyl radical products of radical additions to alkynes are included in Table 2. The unique transition structure for this reaction has a cis-type structure and links to the higher-energy cis alkenyl radical isomer rather than the lower-energy trans isomer. The cis–trans energy differences are 1.1 kJ/mol (where X is H) or 2.9 kJ/mol (where X is CH_3) at the UQCISD/6-31G(d) level of

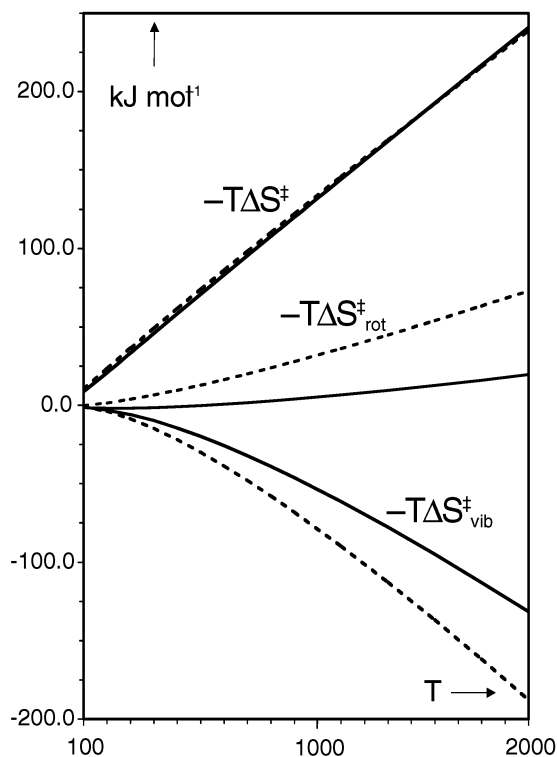


Figure 3. Entropies of activation (plotted as $-T\Delta S^\ddagger$, in kilojoules per mole) and their rotational ($-T\Delta S^\ddagger_{\text{rot}}$) and vibrational ($-T\Delta S^\ddagger_{\text{vib}}$) contributions for methyl radical addition to $\text{CH}\equiv\text{CH}$ (—) and $\text{CH}_2=\text{CH}_2$ (---). Values derived from geometries and frequencies obtained at the UQCISD/6-31G(d) level.

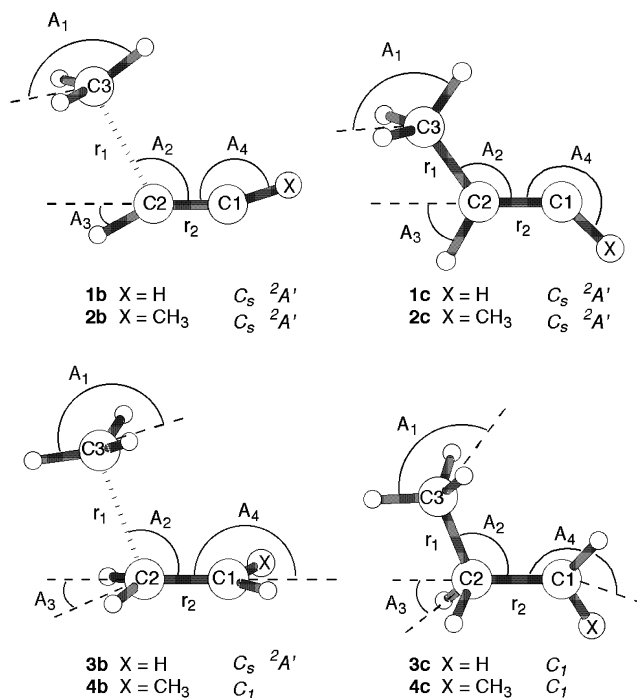


Figure 4. Schematic representation of transition structures and product radicals for methyl radical addition to $\text{CH}\equiv\text{CX}$ and $\text{CH}_2=\text{CHX}$ (where X is H or CH_3). Calculated values for the relevant bond lengths r_1 and r_2 and angles A_1 – A_4 for the transition structure, product radical, and substrate for all four reactions are provided in Table 2.

theory. However, since the barriers to interconversion of the cis and trans forms at this level are just 26.6 kJ/mol (where X is H) or 31.2 kJ/mol (where X is CH_3), we expect that the cis alkenyl radical should ultimately rearrange to the more stable

TABLE 2: Key Geometrical Parameters for the Substrate, Transition Structures, and Product Radicals in Methyl Radical Addition to $\text{CH}=\text{CX}$ and $\text{CH}_2=\text{CHX}$ (where X is H or CH_3)^a

species	r_1	r_2	A_1	A_2	A_3	A_4	
$\text{CH}=\text{CH}$	1a	1.213			0	180	
$^{\bullet}\text{CH}_3$ - - $\text{CH}=\text{CH}$	1b	2.248	1.237	31.1	116.5	29.6	161.7
CH_3 - $\text{CH}=\text{CH}^{\bullet}$ (trans)	1c	1.509	1.321	57.6	125.2	61.3	224.4
CH_3 - $\text{CH}=\text{CH}^{\bullet}$ (cis)	1c'	1.516	1.321	57.7	124.7	60.9	135.6
$\text{CH}=\text{CCH}_3$	2a		1.213			0.0	180.0
$^{\bullet}\text{CH}_3$ - - $\text{CH}=\text{CCH}_3$	2b	2.247	1.237	31.7	115.6	29.6	164.2
CH_3 - $\text{CH}=\text{C}(\text{CH}_3)^{\bullet}$ (trans)	2c	1.508	1.322	57.9	125.4	61.6	222.7
CH_3 - $\text{CH}=\text{C}(\text{CH}_3)^{\bullet}$ (cis)	2c'	1.517	1.323	58.2	125.7	61.3	139.1
$\text{CH}_2=\text{CH}_2$	3a		1.338			0	180
$^{\bullet}\text{CH}_3$ - - $\text{CH}_2=\text{CH}_2$	3b	2.272	1.367	32.5	109.5	18.9	175.0
$\text{CH}_3\text{CH}_2\text{CH}_2^{\bullet}$	3c	1.532	1.497	58.3	112.9	56.0	190.6
$\text{CH}_2=\text{CHCH}_3$	4a		1.339			0.0	180.0
$^{\bullet}\text{CH}_3$ - - $\text{CH}_2=\text{CHCH}_3$	4b	2.276	1.367	32.7	109.2	19.2	174.3
$\text{CH}_3\text{CH}_2\text{CH}(\text{CH}_3)^{\bullet}$	4c	1.531	1.498	58.4	113.3	56.5	196.4

^a Bond lengths (angstroms) and angles (degrees) are based on UQCISD/6-31G(d) optimizations. Geometrical parameters are defined in Figure 4.

trans product. For this reason, all calculated reaction enthalpies in this work relate to the trans form of the alkenyl radical product.

From Table 2, it can be seen that, in keeping with the large exothermicity of the radical addition reactions, the transition structures are early in each case. Where direct comparisons can be made, the transition structures for addition to the double-bonded and triple-bonded substrates show qualitatively similar features. In particular, there are no major differences in the *extents* to which the forming C–C bonds (r_1) and the breaking C≡C and C=C bonds (r_2), the pyramidalization of the attacking methyl group (A_1), and the angle of attack (A_2) have reached their final value in the transition structures. The main geometrical differences between the additions to the alkenes and alkynes relate to the distortion from linearity/planarity at the carbon being attacked and at the remote carbon. In each case, the transition structure for addition to the alkynes is significantly more distorted than for addition to alkenes. At the site of attack, the deviation from linearity/planarity (A_3) is quite similar in the product of addition to either the alkenes or alkynes, but differs significantly (by 10°) in the transition structures. For the remote carbon (which becomes the radical center in the product), the deviation from linearity/planarity (A_4) shows significant differences between the two sets of reactions in both the transition structures and the product radicals. For the alkene addition reactions, distortion from planarity is quite small, amounting to just 10–15° over the course of the reaction. In contrast, the degree of nonlinearity in the addition to alkynes, as measured by the deviation from 180° in A_4 , is quite large (>40°), with 15–20° of this change occurring by the time the transition structure is reached.

In an earlier comparison of methyl radical addition to ethene and ethyne,⁵ the higher barrier for addition to ethyne was attributed to the greater geometrical distortion (and associated deformation energy) required to form the transition structure in this case. These trends are confirmed at the current higher level of theory, for which the respective deformation energies for addition to ethene and ethyne are 18.2 and 25.8 kJ/mol, respectively. The contributions of the unsaturated substrate to these quantities are 11.5 and 19.9 kJ/mol, respectively. The relative deformation energies indicate that, in forming the transition structure for addition to ethyne, the necessary C≡C stretching and C≡C–H bending distortions have a greater energetic cost than the corresponding distortions (i.e., the C=C

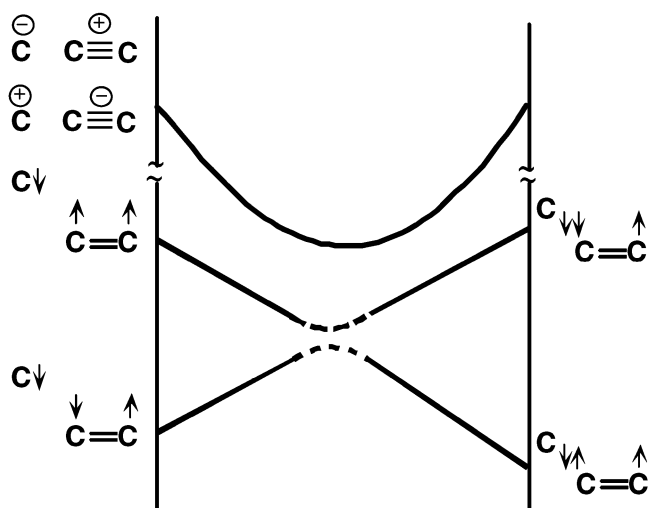
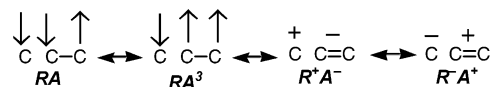


Figure 5. State correlation diagram for radical addition to alkynes showing the variation in energy of the four key configurations as a function of geometry.

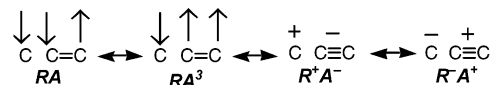
stretch and C=CH₂ wag) in the transition structure for addition to ethene. This in turn would suggest that these distortions are disrupting stronger bonding interactions in the triple-bonded substrate. To provide information about these underlying effects, and to enable a deeper understanding of the relative reactivity of ethene and ethyne toward methyl radical addition, we have carried out an analysis using the curve-crossing model.

Analysis Using the Curve-Crossing Model. The curve-crossing model (also known as the state correlation diagram) was introduced by Shaik and Pross^{13,14} as a qualitative, yet powerful, method for rationalizing trends in reaction barriers in terms of the interaction of the reactant and product electronic configurations, and any other low-lying electronic configurations. This model has previously^{1,34,35} been applied to the analysis of radical addition to alkenes with great success, and in what follows, we use this model to rationalize the differences in radical addition to alkenes and alkynes.

Description of the Model. For radical addition reactions, the key configurations that are considered are the four lowest doublet configurations in the three-electron/three-center system formed from the attacking radical R[•] and the π-bond of the substrate alkene or alkyne (A).^{1,34,35} For addition to alkenes, the configurations are



For the alkyne additions, the analogous configurations are



In each case, the first configuration (RA) corresponds to that of the reactants and the second (RA^3) to that of the products, while the last two (R^+A^- and R^-A^+) are possible charge-transfer configurations which may contribute if they are sufficiently low in energy. The state correlation diagram showing (qualitatively) how the energies of these configurations vary as a function of reaction coordinate for radical additions to alkynes is given in Figure 5.

What Factors Affect the Barrier Height? Applying simple geometric arguments to the state correlation diagram, we can

easily see that the barrier height for radical addition reactions depends on three main factors: the reaction exothermicity (which measures the difference in energy between the reactant and product configurations at their optimal geometries), the singlet–triplet gap in the substrate (which measures the difference in energy between the reactant and product configurations at the reactant geometry), and the relative energies of the possible charge-transfer configurations. The effects of individual variations in these quantities are shown schematically in Figure 6. (For the sake of clarity, we have omitted from these diagrams the adiabatic minimum energy path showing the avoided crossing, as in Figure 5.) It can be seen that the barrier height is lowered by an increase in reaction exothermicity, a decrease in the singlet–triplet gap, or a decrease in the relative energy of one or both of the charge-transfer configurations (provided that these are sufficiently low in energy to contribute to the ground-state wave function).

When Does the Evans–Polanyi Rule Break Down? The observation that the barrier for addition to alkynes is higher than that for addition to alkenes, despite the greater exothermicity of the former reaction, contrasts with a wide variety of chemical reactions for which the Evans–Polanyi rule,^{36,37} which predicts that the barrier height should decrease linearly with increasing exothermicity, is known to hold. In what follows, we use the curve-crossing model to predict two circumstances under which the Evans–Polanyi rule might break down.

The first situation is connected with the relationship between the variation in exothermicity and singlet–triplet gap. Two alternative possibilities are shown in Figure 7. In case a, the singlet–triplet gap decreases as the reaction exothermicity increases. Under these circumstances, it can be seen that the Evans–Polanyi rule would hold (provided of course that charge-transfer interactions are not significant). Such correlations between the singlet–triplet gap and reaction exothermicity are not unreasonable for series of *similar* reactions. Indeed, correlations of this type have been proposed for radical addition to substituted alkenes, as it can be argued that the effect of a substituent both in the triplet state of the alkene and in the final doublet state of the product is related to its ability to stabilize an adjacent unpaired electron.^{1,35} If, however, the substrates are different, then there is no a priori reason to expect such behavior. This leads us to case b in Figure 7, in which the singlet–triplet gap and reaction exothermicity are allowed to vary in opposite directions. Clearly, under these circumstances, the Evans–

Polanyi rule may break down. As drawn in Figure 7b, the increase in the singlet–triplet gap dominates the increase in reaction exothermicity, leading to an increase in the barrier height. Of course, if the increase in singlet–triplet gap is much smaller than the increase in exothermicity, then the latter could dominate and smaller barriers could result. In any case, it can be concluded that if the singlet–triplet gap does not decrease linearly as the reaction exothermicity increases, the Evans–Polanyi rule may not hold.

The second situation under which the Evans–Polanyi rule might be expected to break down is when polar interactions are significant. This can be seen quite clearly in Figure 6c in which two hypothetical reactions having identical singlet–triplet gaps and reaction exothermicities, but different charge-transfer energies, are compared. Provided the charge-transfer configurations are sufficiently low in energy to contribute to the ground-state wave function, any change to their relative energy will alter their stabilizing influence on the transition structure but not the reactants (which, being infinitely separated, cannot interact). Polar interactions can thereby alter the reaction barrier, independent of any change to the reaction exothermicity. Such polar interactions have previously been used to explain deviations from Evans–Polanyi behavior in the addition of strongly electrophilic or nucleophilic radicals to various alkenes,¹ though such effects are not believed to be significant in the specific case of methyl radical addition to ethene, considered in the work presented here (see below).

Curve-Crossing Analysis of Methyl Addition to Alkenes and Alkynes. The above curve-crossing analysis of radical addition reactions leads to the conclusion that the Evans–Polanyi rule would be expected to hold provided that polar interactions are not significant *and* variations in the reaction exothermicity exert either no effect or a proportional effect on the singlet–triplet gap of the substrate. To examine which effects are likely to be responsible for the contrathermodynamic behavior in these reactions, we have calculated the singlet–triplet gaps in the substrates, the relative energies of the charge-transfer configurations, and the net charge on the methyl fragment in the transition structure (see Table 3).

It is clear from Table 3 that the singlet–triplet gap is significantly greater in the alkynes than in the alkenes (by more than 100 kJ/mol) which, as seen in Figure 6b, should lead to an increase in the reaction barrier for the triple-bonded systems. Of course, it was seen in Table 1 that the reaction exothermicity

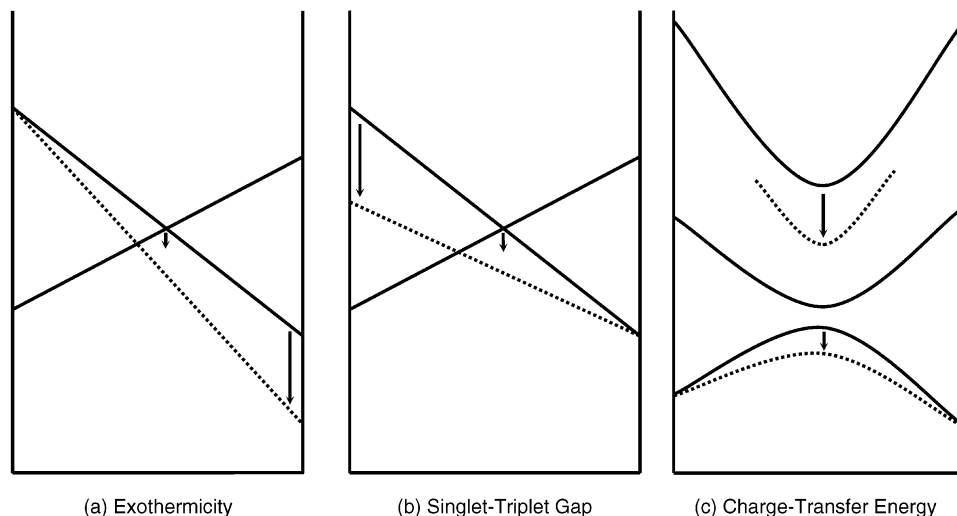


Figure 6. State correlation diagrams showing separately the qualitative effects of (a) increasing the reaction exothermicity, (b) decreasing the singlet–triplet gap, and (c) decreasing the energy of the charge-transfer configuration.

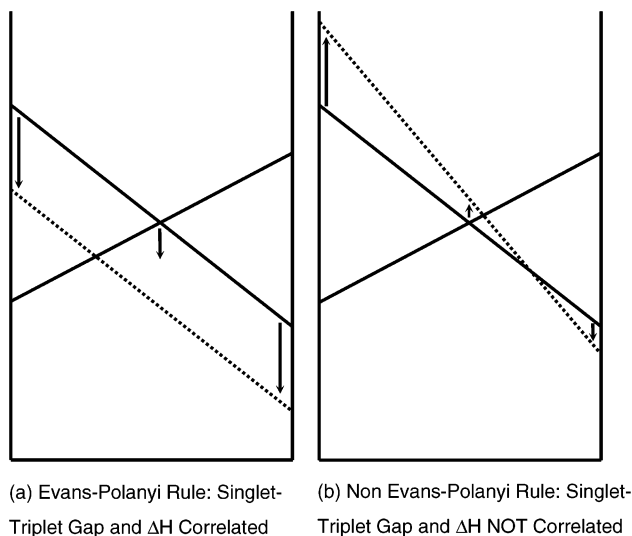


Figure 7. State correlation diagrams showing qualitatively the combined effects on the barrier height of the singlet–triplet gap and the reaction exothermicity when (a) these quantities are correlated with one another and (b) they oppose one another. In case a, the Evans–Polanyi rule would be expected to hold, while in case b, it would not.

TABLE 3: Calculated Relative Energies (electronvolts) of the Triplet Substrate (RA^3)^a and of the Charge-Transfer Configurations (R^+A^- and R^-A^+)^b in Methyl Radical (R) Addition to $CH\equiv CX$ and $CH_2=CHX$ (where X is H or CH_3) and Bader Charges (q) on $\cdot CH_3$ in the Corresponding Transition Structures

reaction	RA^3	R^+A^-	R^-A^+	$q(\cdot CH_3)$
$\cdot CH_3 + CH\equiv CH \rightarrow CH_3CH=CH\cdot$	5.84	11.01	11.73	+0.002
$\cdot CH_3 + CH\equiv CCH_3 \rightarrow CH_3CH=C(CH_3)\cdot$	5.93	10.85	10.80	-0.010
$\cdot CH_3 + CH_2=CH_2 \rightarrow CH_3CH_2CH_2\cdot$	4.65	10.85	10.97	-0.015
$\cdot CH_3 + CH_2=CHCH_3 \rightarrow CH_3CH_2CH(CH_3)\cdot$	4.67	10.53	10.28	-0.024

^a Calculated for a vertical transition at the G3X(MP2)-RAD level.

^b Calculated from the vertical ionization energy (IE) of the donor and vertical electron affinity (EA) of the acceptor molecule at the G3X(MP2)-RAD level. The respective IE and EA values are 9.83 and -0.12 eV for $\cdot CH_3$, 11.61 and -1.19 for $CH\equiv CH$, 10.68 and -0.71 for $CH\equiv CCH_3$, 10.85 and -1.02 for $CH_2=CH_2$, and 10.16 and -0.17 for $CH_2=CHCH_3$, respectively.

is greater for the alkyne addition reactions (by 6.9 kJ/mol at 298 K), and this should contribute to a lowering of the barrier. The situation is thus analogous to that represented in Figure 7b, where there are two opposing effects. In the present work, the larger barrier for the alkyne systems suggests that the barrier-raising effect of the larger singlet–triplet gap dominates. This may reflect the larger differences in the singlet–triplet gap compared with reaction exothermicity (which, as drawn in Figure 7b, lead to the former dominating), and also the earliness of the transition structures in both reactions.

As in previous studies of radical addition to alkenes,³⁸ an indication of the importance of the charge-transfer configurations is obtained from the difference in the ionization energy of the donor and the electron affinity of the acceptor species. The charge-transfer energies in Table 3 suggest that polar interactions might be expected to be more important in the addition to alkenes than in the addition to alkynes. As seen in Figure 6c, provided these configurations are sufficiently low in energy to contribute to the ground-state wave function, this could also help to account for the lower reaction barrier in the former system. However, for all four reactions, the charge-transfer energies exceed the empirically observed³⁸ threshold of 9–9.5

eV, above which the influence of charge transfer would be expected to be unimportant for radical addition reactions. Indeed, as noted above, previous studies³⁸ concluded that polar interactions are not significant in methyl addition to ethene, and hence, they would not be expected to be significant in the addition to ethyne (which has a higher charge-transfer energy). Furthermore, for both reactions, the charge-transfer energies are lower in the corresponding methyl-substituted systems. Since methyl substitution leads to only a minor lowering of the reaction barrier in both cases (see Table 1), this would also suggest that the influence of polar interactions is relatively small in these systems. Finally, the relatively minor influence of the charge-transfer configurations can also be seen in the small size of the charges carried by the methyl group in the transition structures (see Table 3).

In conclusion, a simple curve-crossing analysis reveals that the higher barrier in methyl radical addition to alkynes compared with that in addition to alkenes can be attributed primarily to the larger singlet–triplet gap in the triple-bonded substrates. This effect is sufficiently large that it outweighs the influence of the reaction exothermicity, which favors addition to the alkynes. However, we might expect that for appropriately substituted alkynes and alkenes, the exothermicity preference for addition to alkynes could be significantly enhanced, which could in turn lead to addition to alkynes being kinetically favored. This might occur if the substrates were substituted with π -electron-donating, σ -electron-withdrawing groups (such as F, OH, or NH_2) that stabilize a double bond (relative to a triple bond), since the double bond occurs in the reactant for addition to alkenes but in the product for addition to alkynes. Addition to alkynes should also be kinetically preferred for alkyne substrates having lower singlet–triplet gaps, such as diacetylene. In addition, our calculated charge-transfer energies suggest that polar effects are not likely to be important in the present work. However, in the more general situation, our results suggest that polar interactions should be more significant in alkene than in alkyne additions. This may become important for the addition of more electrophilic or nucleophilic radicals to alkenes and alkynes, where it would be predicted to enhance further the preference for addition to alkenes over alkynes.

Why Do the Singlet–Triplet Gap and Reaction Exothermicity Act in Opposite Directions? The above analysis suggests that the higher barrier for addition to alkynes compared with that for addition to alkenes is due to the higher singlet–triplet gap in the alkyne substrate, which acts in the opposite direction to and also dominates the reaction enthalpy. At first, this may appear counterintuitive, as it might seem that the factors that decrease the stability of the triplet might also affect the stability of the product radical in a (at least qualitatively) similar manner, leading to a decrease (rather than the observed increase) in the reaction exothermicity. In what follows, we attempt to rationalize the opposing trends in the singlet–triplet gap and reaction exothermicity in radical addition to alkenes and alkynes.

The observation that the singlet–triplet gap is larger in alkynes than in alkenes follows immediately from the shorter $C\equiv C$ bond length in the alkynes. This leads to the triplet repulsion being greater in the vertically excited alkynes than in the alkenes. Of course, in the product geometries, this electron–electron repulsion is not relevant because the unpaired electron at the attacked carbon forms a σ -bond with the unpaired electron of the attacking methyl radical. This may partly explain why the trends in the singlet–triplet gaps and exothermicities oppose one another.

Nonetheless, in line with the previous observations of Gazith and Szwarc⁹ and Nicolaidis and Borden,¹⁰ the larger singlet–triplet gap of the alkynes also reflects a stronger π -bonding interaction in the singlet species, arising from the greater overlap of p – π orbitals in the shorter triple bond. We might expect that the stronger π -bonding interaction should lead to addition to alkynes being *less* rather than more exothermic than addition to alkenes. Two effects may help to explain this counterintuitive result. First, while the shorter bond length in acetylene may well lead to a stronger π -interaction, it also leads to a greater destabilization of the σ -interaction. The respective relative energies of ethane at its equilibrium C–C bond length (1.531 Å), and at those of ethylene (1.331 Å) and acetylene (1.205 Å), are 0.0, 71.1, and 246.0 kJ/mol, respectively, at the G3-(MP2)-RAD level of theory. Hence, the overall thermodynamic cost of breaking the stronger π -interaction in acetylene is counteracted by the relaxation of the σ -bond, and is therefore probably much smaller than the trends in the singlet–triplet gaps would suggest. Second, while the singlet–triplet gaps are dominated by the strength of the π -bonding in the singlet and the repulsion in the triplet species, the exothermicities depend on several other factors. As a consequence, the π -bond-breaking processes that may thermodynamically favor addition to alkenes over alkynes are counteracted by other effects. In particular, we note that addition to alkynes results in the formation of a C–C σ -bond in a propenyl radical that has more s-character and is thus stronger than the corresponding C–C σ -bond in the propyl radical.

In conclusion, the trends in the singlet–triplet gaps and reaction exothermicities oppose one another because there are *independent* factors influencing the singlet–triplet gaps (such as the repulsion in the triplet) and the reaction exothermicities (such as the strength of the σ -bonds in the reactants and products) that act in opposite directions.

4. Conclusions

In this study, we present high-level calculations of the barriers, exothermicities, and rate constants for methyl radical addition to alkenes and alkynes. These calculations confirm that the reactions are contrathermodynamic, with addition to the alkene being favored despite the alkyne addition having the greater exothermicity. A simple curve-crossing analysis reveals that the larger barrier for addition to alkynes can be primarily attributed to the larger singlet–triplet gap in the triple-bonded systems. This effect, which can be understood in terms of the greater π -overlap in the singlet and electron–electron repulsion in the triplet alkyne, is large enough to outweigh the barrier-lowering influence of the reaction exothermicity, particularly given the early transition structures in these reactions.

Acknowledgment. We gratefully acknowledge generous allocations of computing time on the Compaq Alphaserver of the National Facility of the Australian Partnership for Advanced Computing and the Australian National University Supercomputing Facility, and provision of a CONACyT–México postdoctoral fellowship (to R.G.-B.), an Australian Research Council (ARC) postdoctoral fellowship (to M.L.C.), and an ARC Discovery grant (to L.R.).

Supporting Information Available: GAUSSIAN archive entries showing UQCISD/6-31G(d) geometries for all species considered in this work (Table S1) and corresponding W1h//QCISD/6-31G(d) total energies (Table S2). This material is available free of charge via the Internet at <http://pubs.acs.org>.

References and Notes

- (1) Fischer, H.; Radom, L. *Angew. Chem., Int. Ed.* **2001**, *40*, 1340–1371.
- (2) A comprehensive list of references to theoretical studies of radical additions to unsaturated systems may be found in ref 1. Representative references from that list and more recent references include the following: (a) Houk, K. N.; Paddon-Row, M. N.; Spellmeyer, D. C.; Rondan, N. G.; Nagase, S. *J. Org. Chem.* **1986**, *51*, 2874–2879. (b) Arnaud, R.; Subra, R.; Barone, V.; Lelj, F.; Olivella, S.; Sole, A.; Russo, N. *J. Chem. Soc., Perkin Trans. 2* **1986**, 1517–1524. (c) Fueno, T.; Kamachi, M. *Macromolecules* **1988**, *21*, 908–912. (d) Gonzales, C.; Sosa, C.; Schlegel, H. B. *J. Phys. Chem.* **1989**, *93*, 2435–2440. (e) Zipse, H.; He, J.; Houk, K. N.; Giese, B. *J. Am. Chem. Soc.* **1991**, *113*, 4324–4325. (f) Wong, M. W.; Pross, A.; Radom, L. *J. Am. Chem. Soc.* **1994**, *116*, 11938–11944. (g) Davis, T. P.; Rogers, S. C. *Macromol. Theory Simul.* **1994**, *3*, 905–913. (h) Wong, M. W.; Radom, L. *J. Phys. Chem.* **1995**, *99*, 8582–8588. (i) Heuts, J. P. A.; Radom, L.; Gilbert, R. G. *Macromolecules* **1995**, *28*, 8771–8781. (j) Bottoni, A. *J. Chem. Soc., Perkin Trans. 2* **1996**, 2041–2047. (k) Wong, M. W.; Radom, L. *J. Phys. Chem. A* **1998**, *102*, 2237–2245. (l) Coote, M. L.; Davis, T. P.; Radom, L. *Macromolecules* **1999**, *32*, 2935–2940. (m) Van Speybroeck, V.; Van Neck, D.; Waroquier, M.; Wauters, S.; Saeys, M.; Marin, G. B. *J. Phys. Chem. A* **2000**, *104*, 10939–10950. (n) Olivella, S.; Bofill, J. M.; Sole, A. *Chem. Eur. J.* **2001**, *7*, 3377–3386. (o) Coote, M. L.; Wood, G. P. F.; Radom, L. *J. Phys. Chem. A* **2002**, *106*, 12124–12138. (p) Hippler, H.; Viskolcz, B. *Phys. Chem. Chem. Phys.* **2002**, *4*, 4663–4668. (q) Leach, A. G.; Wang, R.; Wohlhieter, G. E.; Khan, S. I.; Jung, M. E.; Houk, K. N. *J. Am. Chem. Soc.* **2003**, *125*, 4271–4278. (r) Van Speybroeck, V.; Van Neck, D.; Waroquier, M.; Wauters, S.; Saeys, M.; Marin, G. B. *Int. J. Quantum Chem.* **2003**, *91*, 384–388. (s) Coote, M. L.; Radom, L. *J. Am. Chem. Soc.* **2003**, *125*, 1490–1491.
- (3) Zytowski, T.; Fischer, H. *J. Am. Chem. Soc.* **1997**, *119*, 12869–12878.
- (4) Holt, P. M.; Kerr, J. A. *Int. J. Chem. Kinet.* **1977**, *9*, 185–200.
- (5) Barone, V.; Orlandini, L. *Chem. Phys. Lett.* **1995**, *246*, 45–52.
- (6) Arnaud, R.; Barone, V.; Olivella, S.; Sole, A. *Chem. Phys. Lett.* **1985**, *118*, 573–579.
- (7) Ho, P.; Melius, C. F. *J. Phys. Chem.* **1990**, *94*, 5120–5127.
- (8) Diau, E. W.; Lin, M. C.; Melius, C. F. *J. Chem. Phys.* **1994**, *101*, 3923–3927.
- (9) Gazith, M.; Szwarc, M. *J. Am. Chem. Soc.* **1957**, *79*, 3339–3343.
- (10) Nicolaidis, A.; Borden, W. T. *J. Am. Chem. Soc.* **1991**, *113*, 6750–6755.
- (11) Morokuma, K. *J. Chem. Phys.* **1971**, *55*, 1236–1244.
- (12) Kitaura, K.; Morokuma, K. *Int. J. Quantum Chem.* **1976**, *10*, 325–340.
- (13) Pross, A. *Adv. Phys. Org. Chem.* **1985**, *21*, 99–196.
- (14) Shaik, S. S. *Prog. Phys. Org. Chem.* **1985**, *15*, 197–337.
- (15) Gómez-Balderas, R.; Coote, M. L.; Henry, D. J.; Radom, L. Manuscript in preparation.
- (16) Hehre, W. J.; Radom, L.; Schleyer, P. v. R.; Pople, J. A. *Ab Initio Molecular Orbital Theory*; Wiley: New York, 1986.
- (17) Koch, W.; Holthausen, M. C. *A Chemist's Guide to Density Functional Theory*; Wiley-VCH: Weinheim, Germany, 2000.
- (18) Frisch, M. J.; Trucks, G. W.; Schlegel, H. B.; Scuseria, G. E.; Robb, M. A.; Cheeseman, J. R.; Zakrzewski, V. G.; Montgomery, J. A., Jr.; Stratmann, R. E.; Burant, J. C.; Dapprich, S.; Millam, J. M.; Daniels, A. D.; Kudin, K. N.; Strain, M. C.; Farkas, O.; Tomasi, J.; Barone, V.; Cossi, M.; Cammi, R.; Mennucci, B.; Pomelli, C.; Adamo, C.; Clifford, S.; Ochterski, J.; Petersson, G. A.; Ayala, P. Y.; Cui, Q.; Morokuma, K.; Malick, D. K.; Rabuck, A. D.; Raghavachari, K.; Foresman, J. B.; Cioslowski, J.; Ortiz, J. V.; Stefanov, B. B.; Liu, G.; Liashenko, A.; Piskorz, P.; Komaromi, I.; Gomperts, R.; Martin, R. L.; Fox, D. J.; Keith, T.; Al-Laham, M. A.; Peng, C. Y.; Nanayakkara, A.; Challacombe, M.; Gill, P. M. W.; Johnson, B.; Chen, W.; Wong, M. W.; Andres, J. L.; Gonzalez, C.; Head-Gordon, M.; Replogle, E. S.; Pople, J. A. *GAUSSIAN 98*; Gaussian, Inc.: Pittsburgh, PA, 1998.
- (19) Werner, H.-J.; Knowles, P. J.; Amos, R. D.; Bernhardsson, A.; Berning, A.; Celani, P.; Cooper, D. L.; Deegan, M. J. O.; Dobbyn, A. J.; Eckert, F.; Hampel, C.; Hetzer, G.; Korona, T.; Lindh, R.; Lloyd, A. W.; McNicholas, S. J.; Manby, F. R.; Meyer, W.; Mura, M. E.; Nicklass, A.; Palmieri, P.; Pitzer, R.; Rauhut, G.; Schütz, M.; Stoll, H.; Stone, A. J.; Tarroni, R.; Thorsteinsson, T. *MOLPRO 2000.6*; University of Birmingham: Birmingham, England, 1999.
- (20) Scott, A. P.; Radom, L. *J. Phys. Chem.* **1996**, *100*, 16502–16513.
- (21) Martin, J. M. L.; Parthiban, S. W1 and W2 theories and their variants: thermochemistry in the kJ/mol accuracy range. In *Quantum Mechanical Prediction of Thermochemical Data*; Cioslowski, J., Ed.; Kluwer-Academic: Dordrecht, The Netherlands, 2001; pp 31–65.
- (22) Martin, J. M. L.; De Oliveira, G. J. *J. Chem. Phys.* **1999**, *111*, 1843–1856.
- (23) Parthiban, S.; Martin, J. M. L. *J. Chem. Phys.* **2001**, *114*, 6014–6029.

- (24) Pitzer, K. S.; Gwinn, W. D. *J. Chem. Phys.* **1942**, *10*, 428–440.
- (25) Li, J. C. M.; Pitzer, K. S. *J. Phys. Chem.* **1956**, *60*, 466–474.
- (26) (a) Nordholm, S.; Bacskay, G. B. *Chem. Phys. Lett.* **1976**, *42*, 253–258. (b) Bacskay, G. B. Unpublished work.
- (27) Heuts, J. P. A.; Gilbert, R. G.; Radom, L. *J. Phys. Chem.* **1996**, *100*, 18997–19006.
- (28) Henry, D. J.; Parkinson, C. J.; Radom, L. *J. Phys. Chem. A* **2002**, *106*, 7927–7936.
- (29) Henry, D. J.; Sullivan, M. B.; Radom, L. *J. Chem. Phys.* **2003**, *118*, 4849–4860.
- (30) See, for example: (a) Bader, R. F. W. *Atoms in Molecules: A Quantum Theory*; Clarendon Press: Oxford, England, 1990. (b) Stefanov, B. B.; Cioslowski, J. R. *J. Comput. Chem.* **1995**, *16*, 1394–1404, and references therein.
- (31) There is often some confusion surrounding the definition of the Arrhenius activation energy (E_a), the internal energy of activation (usually denoted ΔE^\ddagger or ΔU^\ddagger), and the enthalpy of activation (ΔH^\ddagger). At 0 K, these quantities are identical ($E_{a0} = \Delta E^\ddagger_0 = \Delta H^\ddagger_0$), but at non-zero temperatures, these quantities can differ by various multiples of RT . For a gas-phase reaction of molecularity m , the following relation holds: $E_{aT} = \Delta E^\ddagger_T + RT = \Delta H^\ddagger_T + mRT$. For more information, see, for example: Steinfeld, J. I.; Francisco, J. S.; Hase, W. L. *Chemical Kinetics and Dynamics*; Prentice Hall: Englewood Cliffs, NJ, 1989.
- (32) Luo, Y.-R. *Handbook of Bond Dissociation Energies in Organic Compounds*; CRC Press: Boca Raton, FL, 2003.
- (33) Berkowitz, J.; Ellison, G. B.; Gutman, D. *J. Phys. Chem.* **1994**, *98*, 2744–2765.
- (34) Radom, L.; Wong, M. W.; Pross, A. Radical Additions to Alkenes: A Theoretical Perspective. In *Controlled Radical Polymerization*; Matyjaszewski, K., Ed.; American Chemical Society: Washington, DC, 1998; pp 31–49.
- (35) Pross, A. *Theoretical and Physical Principles of Organic Reactivity*; John Wiley & Sons: New York, 1995.
- (36) Evans, M. G.; Gergely, J.; Seaman, E. C. *J. Polym. Sci.* **1948**, *3*, 866–879.
- (37) Evans, M. G. *Discuss. Faraday Soc.* **1947**, *2*, 271–279.
- (38) Wong, M. W.; Pross, A.; Radom, L. *J. Am. Chem. Soc.* **1994**, *116*, 6284–6292.